

Photoemission Signatures of Non-Equilibrium Carrier Dynamics from First Principles

Fabio Caruso,¹ Dino Novko,^{2,3} and Claudia Draxl¹

¹*Institut für Physik and IRIS Adlershof, Humboldt-Universität zu Berlin, Berlin, Germany*

²*Center of Excellence for Advanced Materials and Sensing Devices, Institute of Physics, Zagreb, Croatia*

³*Donostia International Physics Center (DIPC), Donostia-San Sebastián, Spain*

Time- and angle-resolved photoemission spectroscopy (tr-ARPES) constitutes a powerful tool to inspect the dynamics and thermalization of hot carriers. The identification of the processes that drive the dynamics, however, is challenging even for the simplest systems owing to the coexistence of several relaxation mechanisms. Here, we devise a Green's function formalism for predicting the tr-ARPES spectral function and establish the origin of carrier thermalization entirely from first principles. The predictive power of this approach is demonstrated by an excellent agreement with experiments for graphene over time scales ranging from a few tens of femtoseconds up to several picoseconds. Our work provides compelling evidence of a non-equilibrium dynamics dominated by the establishment of a hot-phonon regime.

With the advent of ultra-short light sources, time- and angle-resolved photoemission spectroscopy (tr-ARPES) has emerged as a powerful tool to investigate non-equilibrium many-body phenomena with sub-picosecond resolution [1], providing a new momentum to the investigation of dissipation in photo-excited matter. The time dependence of the transient photoemission intensity encodes information on the relaxation mechanisms of excited electronic and vibronic states, and it provides important information on the ultrafast dynamics of hot carriers.

Overall, the non-equilibrium dynamics of the hot carriers in a pump-probe experiment can be thought of as a three-step process: (i) photoexcitation; (ii) thermalization of the electrons; (iii) energy transfer to the lattice. The interaction with a pump pulse in (i) brings the system to an initial non-equilibrium regime characterized by population inversion, where carriers have been promoted from the valence to the conduction bands. The electron-electron scattering and Auger processes in step (ii) drive the system to a thermalized regime, with the electronic occupations well described by a high-temperature Fermi-Dirac function [2–4]. Finally in step (iii), hot carriers dissipate their energy through the interaction with the lattice, for example, via the scattering with acoustic and optical phonons or impurities. The identification of the scattering processes that drives dissipation in step (iii) is of pivotal importance to engineer longer hot-carrier lifetimes and propagation lengths, however, this challenge is complicated by the coexistence of several competing decay channels.

For graphene, for example, it has been widely debated whether the cooling of the electrons and the establishment of thermal equilibrium with the lattice is governed by *supercollisions* [5–7], namely, impurity-assisted scattering to acoustic phonons [8], or rather by a *hot-phonon* regime [9], a scenario in which electrons scatter more favorably with optical phonons [10, 11], leading to a higher effective temperature for these vibrational modes [12].

First-principles calculations of electron-electron [13]

and electron-phonon [14, 15] interaction may provide an answer to such questions by determining accurately the rate of each scattering mechanism [16]. Even though well-established theoretical tools have emerged to identify the signatures of many-body interactions in ARPES [17–21], their generalization to time-resolved phenomena is not straightforward. Non-equilibrium Green's functions (NEGF) [22–25] are a powerful tool to investigate the time scales immediately after photo-excitation (0–30 fs) [26, 27]. However, the high computational cost [28] of NEGF calculations has thus far hampered their application to longer time scales (30–2000 fs) characteristic of the thermalization between electron and lattice degrees of freedom.

In this Letter, we devise an *ab-initio* field-theoretic scheme, based on many-body theory of electron-phonon coupling [16] and rate equations for the electron-lattice thermalization [12, 29, 30], to predict the tr-ARPES spectral function for systems driven out of equilibrium by the interaction with an ultra-short laser pulse. This approach enables the identification of the leading mechanism that drives the hot-carrier relaxation via interaction with the lattice. The accuracy of this approach is validated by the excellent agreement with experimental data for graphene, for which we report tr-ARPES spectral functions for pump-probe delays ranging from a few tens of femtoseconds up to several picoseconds.

To extend the applicability of many-body theory of electron-phonon coupling to the study of time-dependent phenomena, we start by approximating the occupation of the electronic levels for the out-of-equilibrium state by an ordinary Fermi-Dirac distribution with an effective electronic temperature T_{el} . This assumption greatly simplifies the computational complexity of the problem, as it allows one to resort to the equilibrium Green's function formalism. Its validity, however, is limited to time scales subsequent to the thermalization of electronic degrees of freedom [2]. At shorter timescales, conversely, electrons may be found in a non-thermal regime with occupations pronouncedly different from those provided by

a Fermi-Dirac function. In this regime, NEGF provide a more suitable framework for the description of the non-equilibrium dynamics [26]. In analogy to the electrons, the non-equilibrium phonon population is described by a Bose-Einstein distribution. In order to account for the anisotropy of the electron-phonon interaction we consider two distinct effective temperatures for strongly-coupled (sc) and weakly-coupled (wc) phonons, T_{sc} , and T_{wc} . This separation is key to allow for the establishment of a hot-phonon regime. The separation between weakly and strongly coupled phonons can be rigorously addressed by introducing a cutoff λ_c for the mode-resolved electron-phonon coupling strength $\lambda_{\mathbf{q}\nu}$ at equilibrium, such that modes with $\lambda_{\mathbf{q}\nu} > \lambda_c$ ($\lambda_{\mathbf{q}\nu} < \lambda_c$) are described by T_{sc} (T_{wc}). After interaction with a laser pulse [31], the system's dynamics is governed by the exchange of energy between electrons and phonons via electron-phonon coupling [12, 29], which drives the system back to equilibrium. Within this picture, the time dependence of the effective temperatures T_{el} , T_{sc} , and T_{wc} fully defines the non-equilibrium dynamics of the system, which we obtain via the solution of a three-temperature model (TTM) [6, 12, 32, 33], with all parameters determined from first principles. A more detailed description of this procedure is reported in the Supplemental Material [31].

Within these approximations, the time-dependent non-equilibrium self-energy due to electron-phonon interaction can be expressed as:

$$\Sigma_{n\mathbf{k}}(\omega, \Delta t) = \int \frac{d\mathbf{q}}{\Omega_{\text{BZ}}} \sum_{m\nu} |g_{m\nu}(\mathbf{k}, \mathbf{q})|^2 \times \left[\frac{n_{\mathbf{q}\nu}(\Delta t) + f_{m\mathbf{k}+\mathbf{q}}(\Delta t)}{\hbar\omega - \tilde{\varepsilon}_{m\mathbf{k}+\mathbf{q}} + \hbar\omega_{\mathbf{q}\nu}} + \frac{n_{\mathbf{q}\nu}(\Delta t) + 1 - f_{m\mathbf{k}+\mathbf{q}}(\Delta t)}{\hbar\omega - \tilde{\varepsilon}_{m\mathbf{k}+\mathbf{q}} - \hbar\omega_{\mathbf{q}\nu}} \right]. \quad (1)$$

where $g_{m\nu}(\mathbf{k}, \mathbf{q})$ are electron-phonon coupling matrix elements, $\omega_{\mathbf{q}\nu}$ are the phonon frequencies, and $\tilde{\varepsilon}_{n\mathbf{k}} = \varepsilon_{n\mathbf{k}} + i\eta$, with $\varepsilon_{n\mathbf{k}}$ denoting Bloch energies and η a positive infinitesimal. The time dependence of the self-energy is encoded in the out-of-equilibrium fermionic and bosonic distributions, given by $f_{n\mathbf{k}} = [e^{\varepsilon_{n\mathbf{k}}/k_B T_{el}} + 1]^{-1}$ and $n_{\nu\mathbf{q}} = [e^{\omega_{\nu\mathbf{q}}/k_B T_{\nu}} - 1]^{-1}$, respectively, where $T_{\nu} = T_{sc}$ ($T_{\nu} = T_{wc}$) for the strongly (weakly) coupled modes. The evaluation of Eq. (1) gives access to the time- and momentum-resolved spectral function via

$$A_{\mathbf{k}}(\omega, \Delta t) = 1/\pi \sum_n \text{Im} [\omega - \varepsilon_{n\mathbf{k}} - \Sigma_{n\mathbf{k}}(\omega, \Delta t)]^{-1}, \quad (2)$$

which, within the sudden approximation, is closely related to the tr-ARPES photoelectron current. In the following, we proceed to illustrate the application of this approach to the description of the spectral signatures of non-equilibrium carrier dynamics in tr-ARPES measurements of graphene.

The electronic ground-state properties have been obtained from density-functional theory [34, 35] in the local-density approximation. The Kohn-Sham equations

have been solved within the plane-wave pseudopotential method as implemented in QUANTUM ESPRESSO [36] on a homogeneous $40 \times 40 \times 1$ Monkhorst-Pack momentum grid. Phonon frequencies and eigenvectors have been computed from density-functional perturbation theory [37] on a $16 \times 16 \times 1$ grid. Electron and phonon energies and electron-phonon coupling matrix elements have been interpolated [38] using maximally-localized Wannier functions [39]. The Fan-Migdal self-energy has been calculated with the EPW code [40], and the integral over the phonon momentum in Eq. (1) has been evaluated on a $400 \times 400 \times 1$ grid. p -type doping due to the interaction with the substrate has been accounted for through a rigid shift of the Fermi level by 0.2 eV below the Dirac point, which corresponds to a carrier concentration of around $8 \times 10^{12} \text{ cm}^{-2}$. The spectral function has been multiplied by the Fermi-Dirac distribution and convoluted with a Gaussian function of 130 meV and 0.15 \AA^{-1} widths to account for the finite experimental resolution for energy and momentum, respectively [2].

The electron-phonon coupling strength $\lambda_{\mathbf{q}\nu}$, superimposed as a color code to its phonon dispersion in Fig. 1 (a), is dominated by the electronic coupling to the optical E_{2g} and A'_1 phonons in proximity to the Γ and K points in the Brillouin zone, where $\lambda_{\mathbf{q}\nu} \sim 1$. This suggests the disentanglement of the E_{2g} and A'_1 modes from other lattice vibrations, and thus a description of their thermal population via T_{sc} , whereas T_{wc} is used for the remaining modes. This peculiar anisotropy stems from the limited phase space available for electron-phonon scattering [41], which is characteristic for multi-valley semiconductors and Dirac metals. The preferential coupling to the E_{2g} and A'_1 phonons makes them the most likely dissipation mechanism for photo-excited carriers, a scenario that may lead to the emergence of hot phonons [42], as suggested by recent time-resolved Raman spectroscopy measurements [43–46].

Figures 1 (b) and (c) illustrate the time dependence of the electronic and vibrational effective temperatures obtained from the solution of the TTM, where we considered interaction with 30 fs long Gaussian light pulses of fluences $F = 8$ and 3.46 J/m^2 , respectively. Below, time delays are relative to the pump switch-off ($\Delta t = 0$). The abrupt increase of the electronic temperature T_{el} to 2550 and 1930 K, respectively, at $\Delta t = 0$ marks the photo-excitation of hot-carriers following the interaction with the pump, whereas the subsequent decrease stems from the thermalization of electrons and phonons due to electron-phonon coupling. While the temperature of the strongly-coupled phonons T_{sc} approaches 1500 K, reflecting their primary role in the hot-carrier relaxation, the temperature of the remaining lattice vibrations T_{wc} increases only mildly. The comparison of our results with the experimental electronic temperature T_{el} – extracted from Refs. [2, 6] by fitting a Fermi-Dirac function to the time-resolved (momentum-integrated) photoemission

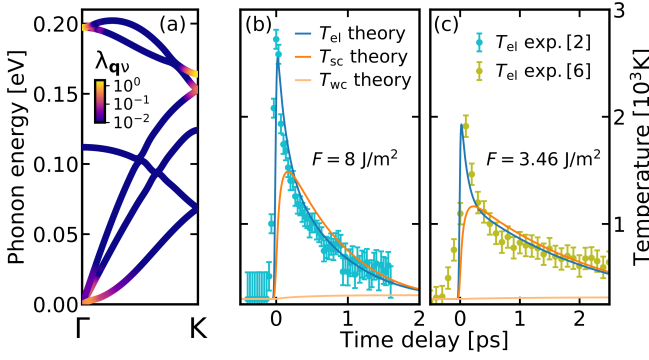


Figure 1. (a) Phonon dispersion and mode- and momentum-resolved electron-phonon coupling strength $\lambda_{q\nu}$ along the $\Gamma - K$ path in the Brillouin zone of graphene. Time dependence of the effective temperatures of electrons T_{el} , strongly coupled optical phonons T_{sc} , and the remaining lattice vibrations T_{wc} , as obtained from the TTM for pump fluences $F = 8 \text{ J/m}^2$ (b) and $F = 3.46 \text{ J/m}^2$ (c). The experimental electron temperatures (dots) are adapted from [2, 6].

signal – is shown in Figs. 1 (b) and (c), and it reveals a remarkable agreement between experiment and theory across the full range of the time delays considered.

Beside validating the TTM for the description of out-of-equilibrium carrier dynamics over time scales ranging from a few tens of femtoseconds to several picoseconds, comparison to experiments suggests that hot-carrier relaxation may be accurately described within the hot-phonon picture, whereby in-plane optical phonons acquire significantly higher effective temperature as compared to other lattice vibrations owing to their higher coupling strength to electrons. Other works reported that hot-carrier relaxation may be dominated by supercollisions [6], impurity-assisted electronic scattering with acoustic phonons. However, it has later been argued that this picture would be incompatible with the low impurity concentrations of graphene [9].

After interaction with the pump, the change of fermionic and bosonic effective temperatures may influence the electron-phonon coupling and its corresponding signatures in spectroscopy. In particular, high values of T_{el} increase the phase space for electron-phonon scattering since, more final states are available for electronic transitions and the thermal phonon population increases with T_{sc} or T_{wc} , enhancing the scattering rate. The interplay of these two trends underpins the time dependence of the electron-phonon interaction. To quantitatively investigate the signatures of these mechanisms in tr-ARPES we proceed to inspect the fingerprints of non-equilibrium carrier dynamics in the time-resolved spectral function.

The tr-ARPES spectral function of *p*-doped graphene, obtained from Eqs. (1) and (2) for a pump fluence $F = 8 \text{ J/m}^2$, is reported in Figs. 2 (b-e) for several time delays. We consider momenta in the immediate vicinity

of the Dirac point, corresponding to the boxed area in Fig. 2 (a), along the high-symmetry line $K-\Gamma$ in the Brillouin zone. We consider the system at room temperature ($T_{el} = T_{sc} = T_{wc} = 300 \text{ K}$) before the interaction with the pump ($\Delta t < 0$). The corresponding spectral function, shown in Fig. 2 (b), is in good agreement with previous studies [47, 48]. The quasiparticle peaks exhibit a finite linewidth resulting from the finite lifetimes of photo-excited holes. The linewidth increases linearly with the electron binding energy, owing to the larger phase space for electron-phonon scattering [49]. The linewidth is much smaller (3-20 meV) than the characteristic energy resolution of tr-ARPES experiments (70-130 meV). Right after interaction with the pump ($\Delta t = 0$), the photo-excitation of the system manifests itself through a partial population of electronic states above the Fermi energy. At a time delay $\Delta t = 0.5 \text{ ps}$ [Fig. 2 (c)] the population of states above the Fermi level decreases, reflecting the partial thermalization of the photo-excited carriers. Finally, for $\Delta t = 2.5 \text{ ps}$ [Fig. 2 (d)] the tr-ARPES spectral function is virtually identical to the one before the pump, indicating that the system has returned to equilibrium.

The relative change in photoemission intensity as a function of time delay – obtained as the difference to the spectral function before the pump [Figs. 2 (f-g)] – provides further insight into the spectral fingerprints of the quasiparticle dynamics in tr-ARPES. The most prominent change in the spectral function results from the enhanced concentration of electrons (holes) above (below) the Fermi surface, induced by the photo-excitation. At zero pump-probe delay [Fig. 2 (f)] the spectral intensity gain (blue) extends up to 1 eV above the Fermi energy, with a corresponding intensity loss (red) for binding energies up to 1 eV. For $\Delta t = 0.5 \text{ ps}$ [Fig. 2 (g)], the gain signal is found only up to the Dirac point, owing to the decrease of T_{el} at larger pump-probe delays. Figure 2 (g) further reveals gain for binding energies larger than 0.3 eV. At variance with the features in the immediate vicinity of the Fermi energy, these features may not be explained in terms of transient electronic temperature, since they extend to energies beyond the domain of thermal temperatures. Conversely, these features reveal a time-dependent renormalization of the quasiparticle energies. This finding is compatible with recent observations in transient optical measurements [50, 51] of narrowing energy gap between the π and π^* bands.

This effect can be quantified by inspecting the change in the real part of the electron self-energy, $\Delta\Sigma = \text{Re}[\Sigma_{n\mathbf{k}}(\varepsilon_{n\mathbf{k}}, \Delta t) - \Sigma_{n\mathbf{k}}^{\text{eq}}(\varepsilon_{n\mathbf{k}})]$, where Σ^{eq} denotes the Fan-Migdal self-energy of the system at equilibrium. $\Delta\Sigma$ provides information pertaining to the time-dependent change of the quasiparticle energies due to electron-phonon interaction. For $\varepsilon_{n\mathbf{k}} = 1 \text{ eV}$, we obtain $\Delta\Sigma = 10 \text{ meV}$ at $\Delta t = 0.5 \text{ ps}$. On the other hand, at $\Delta t = 0 \text{ ps}$, when T_{sc} approaches its maximum value, the quasiparticle energies are almost unchanged ($\Delta\Sigma < 1 \text{ meV}$). This

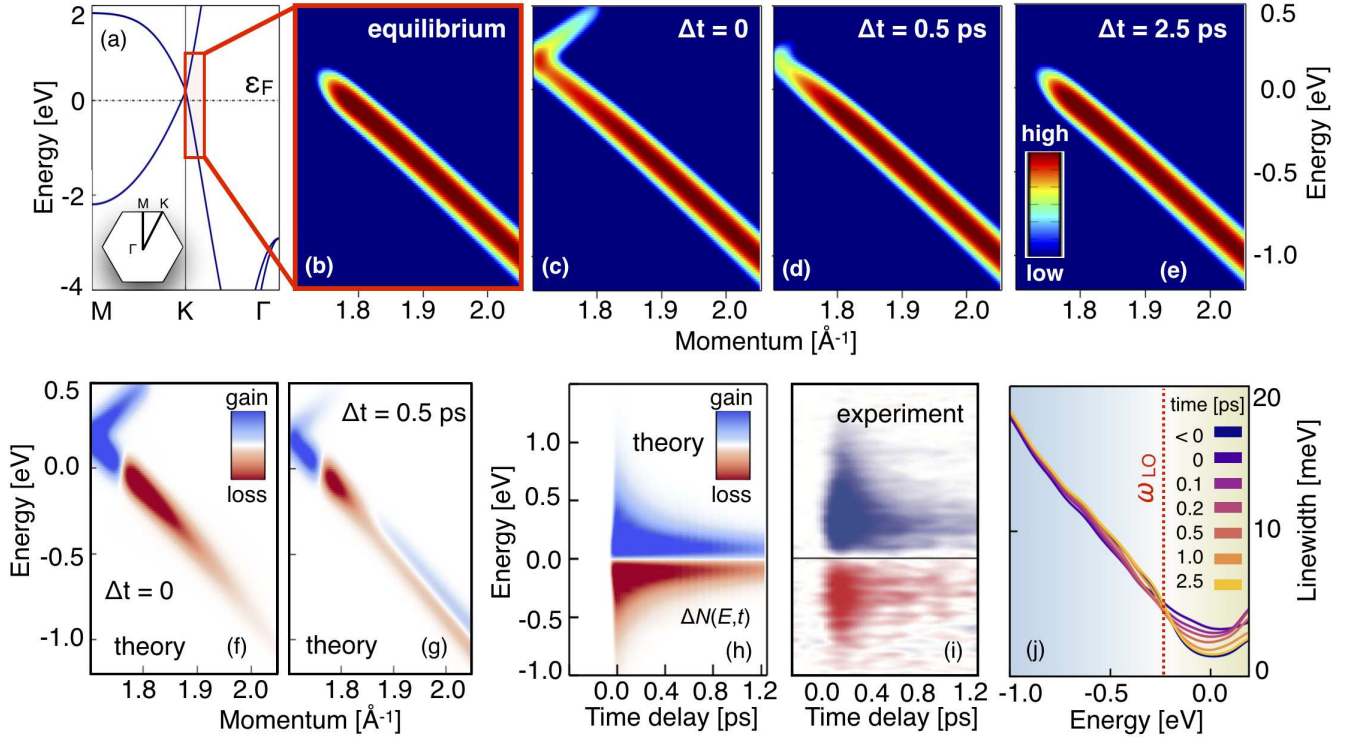


Figure 2. (a) Electron band structure of graphene along the high-symmetry line M-K-Γ in the Brillouin zone (inset) obtained from density-functional theory. Energies are referenced to the Fermi level (dotted line), which is shifted 0.2 eV below the Dirac point to account for p -type doping resulting from the interaction with the substrate. (b-e) Calculated tr-ARPES intensity for crystal momenta close to the Dirac point along K-Γ (red box in panel a) for different time delays between pump and probe beams: before ($\Delta t < 0$) and after ($\Delta t = 0$) pump, during ($\Delta t = 0.5$ ps) and after ($\Delta t = 2.5$ ps) the carrier thermalization. Calculated differential tr-ARPES intensity relative to equilibrium for $\Delta t = 0$ (f) and 0.5 ps (g). Differential pump-probe signal $\Delta N(E, t)$ (integrated over momentum) as obtained from first-principles calculations (h) and from tr-ARPES measurements (i), reproduced from Ref. [2]. (j) Electron linewidths due to electron-phonon interaction at various time delays.

suggests that the energy renormalization (at these lower energies) stems from the electronic coupling to acoustic modes.

To enable the comparison with tr-ARPES measurements across the full range of time delays, we evaluate the differential momentum-integrated pump-probe signal $\Delta N(\omega, \Delta t) = \int d\mathbf{k} [A_{\mathbf{k}}(\omega, \Delta t) - A_{\mathbf{k}}^{\text{eq}}(\omega)]$, where $A_{\mathbf{k}}^{\text{eq}}$ denotes the spectral function at equilibrium. Our calculations for $\Delta N(\omega, \Delta t)$ are reported in Fig. 2 (h), whereas experimental data from [2] are shown in Fig. 2 (i). The comparison with experiment demonstrates good agreement across the full range of time delays.

Finally, we discuss the time dependence of the electron linewidths due to electron-phonon interaction, illustrated in Fig. 2 (j). Close to the Fermi energy, the linewidths exhibit a fast increase after the pump, followed by a slow decrease. After 2.5 ps, the linewidth coincides with the one preceding photo-excitation ($\Delta t < 0$), marking the return to equilibrium. This behavior can be ascribed to the time-dependent change of the phase space for electron-phonon scattering, which is enhanced at high electronic temperatures T_{el} . At binding energies larger than ~ 180 meV, on the other hand, the onset of

strongly-coupled phonons (vertical dotted line) provides an additional scattering channel that underpins the enhancement of linewidth. At these binding energies, the linewidth depend only slightly on time.

As an outlook, a richer scenario of many-body interactions may emerge in compounds characterized by low-energy polar phonons, such as, for example, metal-monochalcogenides (e.g., SnSe, SnS) and transition-metal dichalcogenides (e.g., MoS₂, WS₂). These compounds are good candidates for the observation of spectral fingerprints of hot-phonon dynamics, owing to their large Born effective charges and the preferential coupling to few LO modes. Furthermore, at variance with graphene, the crystal dynamics is characterized by soft lattice vibrations [52, 53] with energies comparable to the room temperature thermal energy (25 meV). Their population may thus be strongly enhanced by the increase of the effective lattice temperature [52], a phenomena that may underpin a strong increase of electron-phonon interaction upon pump. This may lead to the emergence of time-dependent signatures of many-body phenomena in tr-ARPES, such as, transient satellites and kinks.

In conclusions, we have devised a first-principles

scheme to predict transient many-body phenomena in tr-ARPES for systems driven out of equilibrium by the interaction with an ultra-short laser pulse. Based on this approach, we have shown that carrier relaxation in graphene is dominated by the establishment of a hot-phonon regime, whereby in-plane optical phonons provide the primary decay path for photo-excited carriers. The excellent agreement with available experimental data substantiate our findings and the validity of the hot-phonon picture over time scales ranging between a few tens of femtoseconds up to several picoseconds. Overall, this work defines a solid strategy to decipher the quantum mechanical origin of non-equilibrium phenomena in tr-ARPES, paving the way to explore the emergence of transient many-body processes in spectroscopy.

FC and CD gratefully acknowledge financial support from the German Science Foundation (DFG) through the Collaborative Research Center HIOS (SFB 951). DN gratefully acknowledges financial support from the European Regional Development Fund for the Center of Excellence for Advanced Materials and Sensing Devices (Grant No. KK.01.1.1.01.0001) and Donostia International Physics Center (DIPC). Part of the computational resources were provided by the DIPC computing center.

-
- [1] D. N. Basov, M. M. Fogler, A. Lanzara, F. Wang, and Y. Zhang, *Rev. Mod. Phys.* **86**, 959 (2014).
 - [2] I. Gierz, J. C. Petersen, M. Mitrano, C. Cacho, I. C. E. Turcu, E. Springate, A. Stöhr, A. Köhler, U. Starke, and A. Cavalleri, *Nature Mater.* **12**, 1119 (2013).
 - [3] I. Gierz, S. Link, U. Starke, and A. Cavalleri, *Faraday Discuss.* **171**, 311 (2014).
 - [4] T. Li, L. Luo, M. Hupalo, J. Zhang, M. C. Tringides, J. Schmalian, and J. Wang, *Phys. Rev. Lett.* **108**, 167401 (2012).
 - [5] J. C. W. Song, M. Y. Reizer, and L. S. Levitov, *Phys. Rev. Lett.* **109**, 106602 (2012).
 - [6] J. C. Johannsen, S. Ulstrup, F. Cilento, A. Crepaldi, M. Zacchigna, C. Cacho, I. C. E. Turcu, E. Springate, F. Fromm, C. Raidel, T. Seyller, F. Parmigiani, M. Grioni, and P. Hofmann, *Phys. Rev. Lett.* **111**, 027403 (2013).
 - [7] J. C. Johannsen, S. Ulstrup, A. Crepaldi, F. Cilento, M. Zacchigna, J. A. Miwa, C. Cacho, R. T. Chapman, E. Springate, F. Fromm, C. Raidel, T. Seyller, P. D. C. King, F. Parmigiani, M. Grioni, and P. Hofmann, *Nano Lett.* **15**, 326 (2015).
 - [8] A. C. Betz, S. H. Jhang, E. Pallecchi, R. Ferreira, G. Feve, J.-M. Berroir, and B. Placais, *Nature Phys.* **6**, 109 (2013).
 - [9] A. Stange, C. Sohrt, L. X. Yang, G. Rohde, K. Janssen, P. Hein, L.-P. Oloff, K. Hanff, K. Rossnagel, and M. Bauer, *Phys. Rev. B* **92**, 184303 (2015).
 - [10] T. Kampfrath, L. Perfetti, F. Schapper, C. Frischkorn, and M. Wolf, *Phys. Rev. Lett.* **95**, 187403 (2005).
 - [11] S. Butscher, F. Milde, M. Hirtschulz, E. Mali, and A. Knorr, *Appl. Phys. Lett.* **91**, 203103 (2007).
 - [12] P. B. Allen, *Phys. Rev. Lett.* **59**, 1460 (1987).
 - [13] L. Hedin, *Phys. Rev.* **139**, A796 (1965).
 - [14] J. M. Ziman, *Electrons and phonons: the theory of transport phenomena* (Clarendon Press, Oxford, 1960).
 - [15] G. Grimvall, *Electron-phonon interaction in metallic systems* (EPFL, Lausanne, 1988).
 - [16] F. Giustino, *Rev. Mod. Phys.* **89**, 015003 (2017).
 - [17] F. Aryasetiawan, L. Hedin, and K. Karlsson, *Phys. Rev. Lett.* **77**, 2268 (1996).
 - [18] M. Guzzo, G. Lani, F. Sottile, P. Romaniello, M. Gatti, J. J. Kas, J. J. Rehr, M. G. Silly, F. Sirotti, and L. Reininger, *Phys. Rev. Lett.* **107**, 166401 (2011).
 - [19] F. Caruso, H. Lambert, and F. Giustino, *Phys. Rev. Lett.* **114**, 146404 (2015).
 - [20] B. Gumhalter, V. Kovač, F. Caruso, H. Lambert, and F. Giustino, *Phys. Rev. B* **94**, 035103 (2016).
 - [21] C. Verdi, F. Caruso, and F. Giustino, *Nat. Commun.* **8**, 15769 (2017).
 - [22] A. Marini, *Journal of Physics: Conference Series* **427**, 012003 (2013).
 - [23] D. Sangalli and A. Marini, *EPL (Europhysics Letters)* **110**, 47004 (2015).
 - [24] A. Molina-Sánchez, D. Sangalli, L. Wirtz, and A. Marini, *Nano Lett.* **17**, 4549 (2017).
 - [25] M. Bonitz, *Quantum kinetic theory* (Springer, Berlin, 2016).
 - [26] M. Bonitz, K. Balzer, N. Schlünzen, M. R. Rasmussen, and J.-P. Joost, *Phys. Status Solidi B* **0**, 1800490.
 - [27] K. Balzer, M. R. Rasmussen, N. Schlünzen, J.-P. Joost, and M. Bonitz, *Phys. Rev. Lett.* **121**, 267602 (2018).
 - [28] K. Balzer and M. Bonitz, *Nonequilibrium Green's functions approach to inhomogeneous systems* (Springer, Berlin, 2013).
 - [29] Z. Lin, L. V. Zhitilei, and V. Celli, *Phys. Rev. B* **77**, 075133 (2008).
 - [30] D. Novko, J. C. Tremblay, M. Alducin, and J. I. Juaristi, *Phys. Rev. Lett.* **122**, 016806 (2019).
 - [31] See Supplemental Material at [tobeaddedbypublisher](#).
 - [32] L. Perfetti, P. A. Loukakos, M. Lisowski, U. Bovensiepen, H. Eisaki, and M. Wolf, *Phys. Rev. Lett.* **99**, 197001 (2007).
 - [33] C. H. Lui, K. F. Mak, J. Shan, and T. F. Heinz, *Phys. Rev. Lett.* **105**, 127404 (2010).
 - [34] P. Hohenberg and W. Kohn, *Phys. Rev.* **136**, B864 (1964).
 - [35] W. Kohn and L. J. Sham, *Phys. Rev.* **140**, A1133 (1965).
 - [36] P. Giannozzi, S. Baroni, N. Bonini, M. Calandra, R. Car, C. Cavazzoni, D. Ceresoli, G. L. Chiarotti, M. Cococcioni, I. Dabo, and *et al.*, *J. Phys.: Cond. Matter* **21**, 395502 (2009).
 - [37] S. Baroni, S. de Gironcoli, A. Dal Corso, and P. Giannozzi, *Rev. Mod. Phys.* **73**, 515 (2001).
 - [38] F. Giustino, M. L. Cohen, and S. G. Louie, *Phys. Rev. B* **76**, 165108 (2007).
 - [39] N. Marzari, A. A. Mostofi, J. R. Yates, I. Souza, and D. Vanderbilt, *Rev. Mod. Phys.* **84**, 1419 (2012).
 - [40] S. Poncé, E. Margine, C. Verdi, and F. Giustino, *Comp. Phys. Commun.* **209**, 116 (2016).
 - [41] S. Piscanec, M. Lazzeri, F. Mauri, A. C. Ferrari, and J. Robertson, *Phys. Rev. Lett.* **93**, 185503 (2004).
 - [42] H. Wang, J. H. Strait, P. A. George, S. Shivaraman, V. B. Shields, M. Chandrashekhara, J. Hwang, F. Rana, M. G. Spencer, C. S. Ruiz-Vargas, and J. Park, *Appl. Phys. Lett.* **96**, 081917 (2010).
 - [43] D.-H. Chae, B. Krauss, K. von Klitzing, and J. H. Smet,

- Nano Lett. **10**, 466 (2010).
- [44] S. Berciaud, M. Y. Han, K. F. Mak, L. E. Brus, P. Kim, and T. F. Heinz, Phys. Rev. Lett. **104**, 227401 (2010).
 - [45] S. Wu, W.-T. Liu, X. Liang, P. J. Schuck, F. Wang, Y. R. Shen, and M. Salmeron, Nano Lett. **12**, 5495 (2012).
 - [46] C. Ferrante, A. Virga, L. Benfatto, M. Martinati, D. De Fazio, U. Sassi, C. Fasolato, A. K. Ott, P. Postorino, D. Yoon, G. Cerullo, F. Mauri, A. C. Ferrari, and T. Scopigno, Nat. Commun. **9**, 308 (2018).
 - [47] C.-H. Park, F. Giustino, J. L. McChesney, A. Bostwick, T. Ohta, E. Rotenberg, M. L. Cohen, and S. G. Louie, Phys. Rev. B **77**, 113410 (2008).
 - [48] C.-H. Park, F. Giustino, C. D. Spataru, M. L. Cohen, and S. G. Louie, Nano Lett. **9**, 4234 (2009).
 - [49] C.-H. Park, F. Giustino, C. D. Spataru, M. L. Cohen, and S. G. Louie, Phys. Rev. Lett. **102**, 076803 (2009).
 - [50] S. Pagliara, G. Galimberti, S. Mor, M. Montagnese, G. Ferrini, M. S. Grandi, P. Galinetto, and F. Parmigiani, Journal of the American Chemical Society **133**, 6318 (2011).
 - [51] A. T. Roberts, R. Binder, N. H. Kwong, D. Golla, D. Cormode, B. J. LeRoy, H. O. Everitt, and A. Sandhu, Phys. Rev. Lett. **112**, 187401 (2014).
 - [52] F. Caruso, M. Troppenz, S. Rigamonti, and C. Draxl, Phys. Rev. B **99**, 081104 (2019).
 - [53] A. Molina-Sánchez and L. Wirtz, Phys. Rev. B **84**, 155413 (2011).